Postprint of: Kumar Jena S., Chakraverty S., Malikan M., Tornabene F.: Effects of Surface Energy and Surface Residual Stresses on Vibro-Thermal Analysis of Chiral, Zigzag, and Armchair Types of SWCNTs Using Refined Beam Theory. MECHANICS BASED DESIGN OF STRUCTURES AND MACHINES, AN INTERNATIONAL JOURNAL. (2020).

Effects of Surface Energy and Surface Residual Stresses on Vibro-Thermal Analysis of Chiral, Zigzag, and Armchair Types of SWCNTs Using Refined Beam Theory

Subrat Kumar Jena[1], S. Chakraverty[2]*, Mohammad Malikan[3], Francesco Tornabene[4]

[1, 2] Department of Mathematics, National Institute of Technology Rourkela, Odisha, 769008, India

[3]Department of Mechanics of Materials and Structures, Faculty of Civil and Environmental Engineering, Gdansk University of Technology, 80-233, ul. G. Narutowicza 11/12, Gdansk, Poland

[4] Department of Innovation Engineering, University of Salento, 73100, Lecca, Italy

*Corresponding author

E-mail:[1] sjena430@gmail.com, [2]sne_chak@yahoo.com, [3] mohammad.malikan@pg.edu.pl, [4]francesco.tornabene@unisalento.it

Abstract

In this article, vibration characteristics of three different types of Single-Walled Carbon Nanotubes (SWCNTs) such as armchair, chiral, and zigzag carbon nanotubes have been investigated considering the effects of surface energy and surface residual stresses. The nanotubes are embedded in the elastic substrate of the Winkler type and are also exposed to low and high-temperature environments. A new refined beam theory namely, one-variable shear deformation beam theory has been combined with Hamilton's principle to develop the governing equations of the proposed model. The size-dependent behavior of the SWCNTs is addressed by Eringen's nonlocal elasticity theory whereas the model is investigated analytically by employing Navier's technique. Also, a parametric study has been conducted to analyze the effects of various scaling parameters such as small scale parameter, temperature change, thermal environments, Winkler modulus, and length of the beam. The results are also validated with previously published articles in special cases witnessing robust agreement.

Keywords

Vibration; SWCNT; Surface Energy; Surface Residual Stresses; Elastic Foundation; Thermal Environment.

1. Introduction

Carbon nanotubes (CNTs), the masterpiece of engineering materials, are of interest for mechanical, chemical, and physical researchers around the world. One of the most significant parameters which define the geometrical structure of these nanotubes can be the chiral angle. The angle can classify the CNTs into three geometrical shapes. In the first case, the angle equals to zero, and so the CNT obeys a zigzag plan in the peripheral direction of the tube. For this reason, this nanotube is so-called zigzag CNTs. For these tubes, some of the carbon-carbon bonds are parallel to the horizontal axis. If the chiral angle equals 30 degrees, the CNT follows an armchair plan in which the CNT is well-known as armchair CNT. For these tubes, some of the carbon-carbon bonds are vertical to the horizontal axis. In another case, the nanotube is called chiral CNT. These geometrical shapes of the nanotubes can be prepared during its producing. Each shape has its own properties and characteristics. Various shapes of CNTs will be of great importance when manufactured on a large scale with controlled properties (Zhang and Li 2009).

The robustness and flexibility of single-walled carbon nanotubes (SWCNTs) give them the potential to be used in the control of other nanometer structures. So they will play an essential role in nanotechnology engineering. Therefore, there have been comprehensive studies on the prediction of their mechanical behavior. Farshi, Assadi, and Alinia-Ziazi (2010) examined the effect of surface for a nanotube exposed to vibrational situations. The nanotube was assumed in the framework of the Timoshenko beam model. They showed that the impact of surface markedly deviates the results of the natural frequency, and such an effect can be significant to embed in the analysis of nanostructures. Murmu and Pradhan (2010) took effects of the thermal environment on the buckling of nanotubes. The nanotube was connected to a polymer matrix, and the nanoscale behavior was simulated by Eringen's nonlocal theory. Lee and Chang (2010) evaluated the effects of the surface on the vibrational behavior of a carbon nanotube based on the kinematic displacement field of the Timoshenko model. Ghavanloo and Fazelzadeh (2012) based on the chirality effect considered free vibrations of SWCNT assuming an anisotropic shell to model the nanotube. The complex method and the Flügge shell theory as analytical methods were utilized. Zhen (2017) examined nonlocal and surface effects on the wave propagation of the nanotubes by considering the Euler-Bernoulli displacement field and internal viscosity impacts into the model. Jiang, Wang, and Zhang (2017) proposed a refined Fourier series in order to examine the natural frequency of Timoshenko CNTs. The beam was bridged on a silicon channel. The results were extracted by using a molecular dynamics simulation method. Hussain et al. (2019) studied the vibration characteristics of armchair and zigzag type of single-walled carbon nanotubes for clamped-clamped and clamped-free boundary conditions by employing Fourier method and nonlocal behavior of the nanotube was addressed by the Eringen's nonlocal theory. In the pioneering work of Semmah et al. (2019), buckling behavior of a zigzag type of single-walled boron nitride nanotube was analyzed analytically by the help of nonlocal first-order shear deformation theory and the nanotube was placed in Winkler elastic foundation which was subjected to the thermal environment. Abualnour et al. (2019), by exploiting a new simple four-variable trigonometric plate theory, investigated the thermo-mechanical bending behavior of antisymmetric cross-ply laminates.

Karami, Janghorban and Tounsi (2019a) studied wave characteristics of nanosize plates composed of anisotropic material using three-dimensional bi-Helmholtz nonlocal strain gradient theory. In the pioneering work of Karami, Janghorban and Tounsi (2019b), nonlocal strain

gradient model was combined with refined plate model to investigate the wave propagation of FG anisotropic nanoplate. Some other important investigation related to functionally graded nanoplate can be found in Karami, Janghorban and Tounsi (2019c) and Karami et al. (2019). Bensattalah et al. (2019) studied buckling characteristics of triple-walled carbon nanotubes embedded in an elastic medium subjected to axial compression. Timoshenko beam theory in conjunction with nonlocal elasticity theory was used to model the governing equation. Bensattalah, Zidour, and Daouadji (2018) investigated free and forced vibration of carbon nanotubes which was placed on an elastic foundation and exposed to the thermal environment. The carbon nanotubes were modeled with nonlocal Euler-Bernoulli beam theory and subjected to dynamical loads. Adim et al. (2016) analyzed the dynamical characteristics of laminated composite plates with the help of an efficient refined shear deformation theory. As per this beam theory, the transverse displacements comprise bending and shear components and the bending components do not add to shear forces whereas the shear components do not contribute to bending moments. Adim and Daouadji (2016) implemented higher-order and normal shear deformation theories to study the effect of thickness of plates made up of functionally graded material.

Belbachir et al. (2019) studied bending response of anti-symmetric cross-ply laminated plates exposing to nonlinear themo-mechanical loading with the help of refined plate theory. Zarga et al. (2019) investigated the bending response of a functionally graded sandwich plate, implementing a quasi-3D shear deformation theory subjected to thermos-mechanical loads. In another work of Mahmoudi et al. (2019), a refined quasi-3D shear deformation theory is used to study thermos-mechanical behavior of a sandwich plate made of functionally graded materials embedded in the elastic foundation. Tlidji et al. (2019) analyzed the free vibration of functionally graded microbeam using a quasi-3D beam theory and by assuming different material distribution function. Some important works related to various nanostructures can be seen in Boutaleb et al. (2019), Alimirzaei et al. (2019), Berghouti et al. (2019) and Medani et al. (2019). The studies on the mechanical analysis of carbon nanotubes are not limited to the mentioned ones and there can be found other important works (Larbi et al. 2013; Malikan 2019; Arefi and Arani 2018; Jena and Chakraverty 2019; Jena, Chakraverty, and Tornabene 2019a, 2019b, 2019c; Jena, Chakraverty, and Jena 2019; Jena, Chakraverty, and Malikan 2019; Jena et al. 2019; Dastjerdi and Tadi Beni 2019; Fattahi, Sahmani, and Ahmed 2019; Bedia et al. 2019; Draoui et al. 2019; Malikan, Krasheninnikov, and

Eremeyev 2020; Malikan and Eremeyev 2020; Jena, Chakraverty, and Malikan 2020a; Jena, Chakraverty, and Malikan 2020b).

As stated in the aforementioned studies and research on the statics and dynamics of the carbon nanotubes, this research seeks to investigate the vibration characteristics of the SWCNTs taking into account three different frameworks, that is, chiral, armchair and zigzag carbon nanotubes subjected to a thermal environment to elucidate the difference between their mechanical response. In addition, the surface effects as a major impact among the nanostructures are here taken into investigation. On the other hand, the nanotubes are embedded in a polymer substrate, namely the Winkler foundation. To predict the motion of the model's nodes, the field of displacements along two axes is utilized as a new refined beam theory, namely, one variable shear deformation beam theory. After formulation, the required vibration equations have been obtained to analyze the pivot-pivot nanotube with numerical results.

2. Proposed model

In this model, a SWCNT having a length L, outer diameter d_o, inner diameter d_i, and wall thickness t are considered. The mechanical properties of the SWCNT are E, ρ, and υ which denote Young's modulus, mass density, and Poisson's ratio, respectively. E_i, and t_i denote Young's modulus and thickness of the inner surface layer whereas E_o, and t_o designate Young's modulus and thickness of the outer surface layer.

In order to study the effects of both the layers, we have assumed that $E_i t_i = E_o t_o$, which is equal to $E_s t_0$ as a material property of the SWCNT. Surface effects which include surface energy and surface residual stresses, influence the dynamical behaviors of nanostructures considerably. Moreover, the surface energy aids in the increase of the flexural rigidity whereas the surface residual stresses act as distributed transverse load. The flexural rigidity or bending rigidity due to surface energy may be stated as (Farshi, Assadi, and Alinia-Ziazi 2010, Zhen 2017, Jena et al. 2019b)

$$(EI)^{se} = \frac{\pi}{8} E_s t_0 \left(d_o^3 + d_i^3\right), \tag{1}$$

Now, the effective flexural rigidity of the nanotube is obtained as (Farshi, Assadi, and Alinia-Ziazi 2010, Zhen 2017, Jena et al. 2019b)

$$(EI)^{eff} = (EI) + (EI)^{se} = (EI) + \frac{\pi}{8} E_s t_0 \left(d_o^3 + d_i^3\right) \tag{2}$$

The distributed transverse load due to surface residual stresses as per the Laplace-Young equation is presented as (Farshi, Assadi, and Alinia-Ziazi 2010, Zhen 2017, Jena et al. 2019b)

$$q(x) = 2\tau\left(d_o + d_i\right)\frac{\partial^2 w}{\partial x^2} \tag{3}$$

Here τ is surface tension due to residual stresses.

The displacement fields, as per new refined beam theory can be expressed as (Malikan, Nguyen, and Tornabene 2018a, Malikan, Dimitri, and Tornabene 2019, Jena et al. 2019b, Jena, Chakraverty, and Malikan 2020)

$$\begin{aligned} u_1(x,z,t) &= u(x,t) - z\frac{\partial w(x,t)}{\partial x} \\ u_2(x,z,t) &= 0 \\ u_3(x,z,t) &= w(x,t) + B\frac{\partial^2 w(x,t)}{\partial x^2} \end{aligned} \tag{4}$$

In which $u(x,t)$ and $w(x,t)$ are the displacements of the neutral axis in axial and transverse directions, respectively. $B = \frac{EI}{AG}$, where E is Young's modulus, $I = \int_A z^2\, dA$ is the moment of area, A is the area of cross-section, and G is the shear modulus. Considering the Von Kármán hypothesis, the strain displacement relations are given as

$$\begin{aligned} \varepsilon_{xx} &= \frac{\partial u}{\partial x} - z\frac{\partial^2 w}{\partial x^2} + \frac{1}{2}\left(B\frac{\partial^3 w}{\partial x^3} + \frac{\partial w}{\partial x}\right)^2 - \alpha_x \Delta T \\ \gamma_{xz} &= B\frac{\partial^3 w}{\partial x^3} \end{aligned} \tag{5}$$

Here $\alpha_x \Delta T$ is the thermal axial strain along the x-axis and α_x is the coefficient of thermal expansion.

The virtual strain energy (δU) may be written as

$$\delta U = \iiint_V \left(\sigma_{xx}\delta\varepsilon_{xx} + \sigma_{xz}\delta\gamma_{xz}\right)dV$$

$$= \int_0^L \left[\begin{array}{l} N_{xx}\dfrac{\partial\delta u}{\partial x} - M_{xx}\dfrac{\partial^2\delta w}{\partial x^2} + Q_{xz}B\dfrac{\partial^3\delta w}{\partial x^3} + \\ N_{xx}\left(B^2\dfrac{\partial^3 w}{\partial x^3}\dfrac{\partial^3\delta w}{\partial x^3} + B\dfrac{\partial^3 w}{\partial x^3}\dfrac{\partial\delta w}{\partial x} + B\dfrac{\partial w}{\partial x}\dfrac{\partial^3\delta w}{\partial x^3} + \dfrac{\partial w}{\partial x}\dfrac{\partial\delta w}{\partial x}\right) \end{array}\right]dx \tag{6}$$

$$= \int_0^L \left[\begin{array}{l} -\dfrac{\partial N_{xx}}{\partial x}\delta u + \dfrac{\partial^2 M_{xx}}{\partial x^2}\delta w - B\dfrac{\partial^3 Q_{xz}}{\partial x^3}\delta w - B^2\left(\dfrac{\partial^3}{\partial x^3}\left(N_{xx}\dfrac{\partial^3 w}{\partial x^3}\right)\right)\delta w \\ -B\left(\dfrac{\partial}{\partial x}\left(N_{xx}\dfrac{\partial^3 w}{\partial x^3}\right)\right)\delta w - B\left(\dfrac{\partial^3}{\partial x^3}\left(N_{xx}\dfrac{\partial w}{\partial x}\right)\right)\delta w - \dfrac{\partial}{\partial x}\left(N_{xx}\dfrac{\partial w}{\partial x}\right)\delta w \end{array}\right]dx$$

where $M_{xx} = \int_A z\sigma_{xx}dA$, $N_{xx} = \int_A \sigma_{xx}dA$, and $Q_{xz} = \int_A \sigma_{xz}dA$ are the local stress resultants of the beam.

The virtual kinetic energy (δT) of the nanotube can be written as

$$\delta T = \rho\iiint_v \left[\left(\frac{\partial u_1}{\partial t}\right)\left(\frac{\partial\delta u_1}{\partial t}\right) + \left(\frac{\partial u_3}{\partial t}\right)\left(\frac{\partial\delta u_3}{\partial t}\right)\right]dV$$

$$= \int_0^L \left[\begin{array}{l} I_0\dfrac{\partial u}{\partial t}\dfrac{\partial\delta u}{\partial t} + I_2\dfrac{\partial^2 w}{\partial x\partial t}\dfrac{\partial^2\delta w}{\partial x\partial t} + I_0\dfrac{\partial w}{\partial t}\dfrac{\partial\delta w}{\partial t} + \\ I_0 B\dfrac{\partial w}{\partial t}\dfrac{\partial^3\delta w}{\partial x^2\partial t} + I_0 B\dfrac{\partial^3 w}{\partial x^2\partial t}\dfrac{\partial\delta w}{\partial t} + I_0 B^2\dfrac{\partial^3 w}{\partial x^2\partial t}\dfrac{\partial^3\delta w}{\partial x^2\partial t} \end{array}\right]dx \tag{7}$$

$$= \int_0^L \left[-I_0\frac{\partial^2 u}{\partial t^2}\delta u - \left(I_2\frac{\partial^4 w}{\partial x^2\partial t^2} + I_0\frac{\partial^2 w}{\partial t^2} + 2I_0 B\frac{\partial^4 w}{\partial x^2\partial t^2} + B^2 I_0\frac{\partial^6 w}{\partial x^4\partial t^2}\right)\delta w\right]dx$$

In which $I_0 = \rho A$ and $I_2 = \rho I$, are called mass moments of inertia.

The virtual work done (δW) by external loads is defined as

$$\delta W = \int_0^L \left[2\tau\left(d_o + d_i\right)\left(\frac{\partial^2 w}{\partial x^2}\right) - k_w w - \left(\frac{EA\alpha_x}{1-2\nu}\Delta T\right)\left(\frac{\partial^2 w}{\partial x^2}\right)\right]\delta w dx, \tag{8}$$

where k_w is the Winkler modulus, α_x is the coefficient of thermal expansion, ΔT is the change in temperature, and ν is the Poisson's ratio of the nanotube.

Substituting Eqs. (6-8) in Hamilton's principle $\delta\prod = \int_0^t \delta\left(T-\left(U+W\right)\right)dt,$ and neglecting the in-plane force resultant $\left(N_{xx}\right)$ (linear free vibration) we obtain the equations of motion as

$$\begin{bmatrix} -\frac{\partial^2 M_{xx}}{\partial x^2}+B\frac{\partial^3 Q_{xz}}{\partial x^3}-2\tau\left(d_o+d_i\right)\left(\frac{\partial^2 w}{\partial x^2}\right)+\left(\frac{EA\alpha_x}{1-2\nu}\Delta T\right)\left(\frac{\partial^2 w}{\partial x^2}\right) \\ +k_w w-I_2\frac{\partial^4 w}{\partial x^2\partial t^2}-I_0\left(\frac{\partial^2 w}{\partial t^2}+2B\frac{\partial^4 w}{\partial x^2\partial t^2}+B^2\frac{\partial^6 w}{\partial x^4\partial t^2}\right) \end{bmatrix}=0 \tag{9}$$

The local stress resultants, using Hookean stress-strain elasticity relation can be rewritten as

$$\begin{aligned} M_{xx} &= -EI\frac{\partial^2 w}{\partial x^2} \\ Q_{xz} &= AGB\frac{\partial^3 w}{\partial x^3} \end{aligned} \tag{10}$$

From the Eringen's nonlocal elasticity theory, we have (Malikan 2019)

$$\left(1-\left(e_0 a\right)^2\frac{\partial^2}{\partial x^2}\right)\sigma_{ij}=C_{ijkl}\varepsilon_{kl} \tag{11}$$

In which $\sigma_{ij},\varepsilon_{kl}$ and C_{ijkl} are stress tensor, strain tensor and elastic modulus constant, respectively.

From Eq. (10) and Eq. (11), the nonlocal stress resultants may be expressed as

$$\left(1-\left(e_0 a\right)^2\frac{\partial^2}{\partial x^2}\right)M_{xx}=-EI\frac{\partial^2 w}{\partial x^2} \tag{12.a}$$

$$\left(1-\left(e_0 a\right)^2\frac{\partial^2}{\partial x^2}\right)Q_{xz}=AGB\frac{\partial^3 w}{\partial x^3} \tag{12.b}$$

Implementing Eq. (12) in Eq. (9), the governing equation of motion is expressed as

$$\left(1-\left(e_0 a\right)^2\frac{\partial^2}{\partial x^2}\right)\begin{bmatrix} 2\tau\left(d_o+d_i\right)\left(\frac{\partial^2 w}{\partial x^2}\right)-\left(\frac{EA\alpha_x}{1-2\nu}\Delta T\right)\left(\frac{\partial^2 w}{\partial x^2}\right) \\ -k_w w+I_2\left(\frac{\partial^4 w}{\partial x^2\partial t^2}\right)+I_0\begin{pmatrix}\frac{\partial^2 w}{\partial t^2}+2B\frac{\partial^4 w}{\partial x^2\partial t^2} \\ +B^2\frac{\partial^6 w}{\partial x^4\partial t^2}\end{pmatrix}\end{bmatrix}=EI\frac{\partial^4 w}{\partial x^4}+AGB^2\frac{\partial^6 w}{\partial x^6} \quad (13)$$

Considering the surface energy, i.e. Eq. (2) in the Eq. (13), we obtain the governing equation of motion as

$$\left(1-\left(e_0 a\right)^2\frac{\partial^2}{\partial x^2}\right)\begin{bmatrix} 2\tau\left(d_o+d_i\right)\left(\frac{\partial^2 w}{\partial x^2}\right)-\left(\frac{EA\alpha_x}{1-2\nu}\Delta T\right)\left(\frac{\partial^2 w}{\partial x^2}\right)- \\ k_w w+I_2\left(\frac{\partial^4 w}{\partial x^2\partial t^2}\right)+I_0\begin{pmatrix}\frac{\partial^2 w}{\partial t^2}+2B^*\frac{\partial^4 w}{\partial x^2\partial t^2} \\ +B^{*2}\frac{\partial^6 w}{\partial x^4\partial t^2}\end{pmatrix}\end{bmatrix}=\left(EI\right)^{eff}\frac{\partial^4 w}{\partial x^4}+AGB^{*2}\frac{\partial^6 w}{\partial x^6} \quad (14)$$

In which $B^*=\frac{\left(EI\right)^{eff}}{AG}$ and $\left(EI\right)^{eff}=\left(EI\right)+\left(EI\right)^{se}$, where $\left(EI\right)^{se}$ is the flexural rigidity due to surface energy.

3. Analytical Method

The Navier's method has been used to solve the governing equation analytically for Simply Supported boundary condition. According to Navier's approach, the transverse displacement $\left(w\right)$ may be expressed as (Malikan, Nguyen, and Tornabene 2018, Malikan, Dimitri, and Tornabene 2019, Jena et al. 2019b, Jena, Chakraverty, and Malikan 2020)

$$w\left(x,t\right)=\sum_{n=1}^{\infty}W_n\sin\left(\frac{n\pi}{L}x\right)e^{i\omega_n t} \quad (15)$$

In which W_n, and ω_n are the displacement and frequency of the beam.

Plugging Eq. (15) in Eq. (14), the frequency parameter $\left(\omega^2\right)$ may be stated as

$$\omega_n^2 = \frac{\begin{array}{c} 2\tau(d_o+d_i)\left(\frac{n\pi}{L}\right)^2 + 2\tau(d_o+d_i)(e_0a)^2\left(\frac{n\pi}{L}\right)^4 + k_w + (e_0a)^2 k_w\left(\frac{n\pi}{L}\right)^2 \\ -\left(\frac{EA\alpha_x}{1-2\nu}\Delta T\right)\left(\frac{n\pi}{L}\right)^2 - \left(\frac{EA\alpha_x}{1-2\nu}\Delta T\right)(e_0a)^2\left(\frac{n\pi}{L}\right)^4 + (EI)^{eff}\left(\frac{n\pi}{L}\right)^4 - AGB^{*2}\left(\frac{n\pi}{L}\right)^6 \end{array}}{\begin{array}{c} \left\langle I_2\left(\frac{n\pi}{L}\right)^2 - I_0 + 2B^* I_0\left(\frac{n\pi}{L}\right)^2 - B^{*2} I_0\left(\frac{n\pi}{L}\right)^4 \right\rangle + (e_0a)^2 \\ \left\langle I_2\left(\frac{n\pi}{L}\right)^4 - I_0\left(\frac{n\pi}{L}\right)^2 + 2B^* I_0\left(\frac{n\pi}{L}\right)^4 - B^{*2} I_0\left(\frac{n\pi}{L}\right)^6 \right\rangle \end{array}} \quad (16)$$

4. Results and discussion

Three different types of SWCNTs have been considered in this study which include zigzag, chiral and armchair nanotubes. The diameters of the nanotubes with chirality indices $(n,\ m)$ are given by Zhen (2017) $d = \frac{a}{\pi}\sqrt{3(n^2+m^2+mn)}$, where '$a$' is the internal characteristics length or C-C bond length which is equal to $0.142nm$. In this regard, we have considered zigzag nanotube with chirality indices $(21,\ 0)$ and the corresponding diameter is $d = 1.64nm$, the chiral nanotube is having chirality indices $(18,\ 9)$ with diameter $d = 1.86nm$ whereas the chirality indices of the armchair nanotube are assumed as $(16,\ 16)$ with diameter $d = 2.17nm$. The natural frequencies (ω) and critical buckling loads (P_{cr}) for the above-mentioned SWCNTs have calculated by implementing Navier's methods for Hinged-Hinged (H-H) boundary condition. Further, for the parametric study, we have been considered (Zhen 2017) Young's modulus $E = 1TPa$, the wall thickness of the nanotube $t = 0.34nm$, the mass density $\rho = 1370Kg/m^3$, surface tension due to residual stresses $\tau = 0.31N/m$, Poisson's ratio $\nu = 0.19$ and $E_s t_0 = 35.3N/m$

4.1 Validation

For validation purpose of the present model, surface effects which includes surface energy and surface tension due to residual stresses, thermal environment, elastic foundation, and B^* are neglected and the results for fundamental frequencies of Pined-Pined (P-P) boundary condition are compared with Reddy (2007), Jena and Chakraverty (2018) which is demonstrated in Table 1, witnessing robust agreement.

Table 1 Validation of non-dimensional frequency parameters with Reddy (2007), Jena and Chakraverty (2018).

$(e_0a)^2$	0	1	2	3	4
Present	9.8696	9.4159	9.0195	8.6693	8.3569
Reddy (2007)	9.8696	9.4159	9.0195	8.6693	8.3569
Jena and Chakraverty (2018)	9.8696	9.4159	9.0195	8.6693	8.3569

4.2 Influence of small scale parameter

This subsection is devoted to studying the impacts of small scale parameter (e_0a) on frequency parameters $\left(\lambda_n = \omega_n L^2 \sqrt{\frac{\rho A}{(EI)^{eff}}}\right)$ which are presented in Figs. 1-2. For this purpose, $k_w = 1GPa$, $L = 10nm$, and $\Delta T = 100K$ are taken into consideration along with other parameters mentioned in results and discussion subsection. First and second mode frequency parameters of armchair, chiral, and zigzag CNTs are taken into study considering both the low and high-temperature environments. It may also be noted that for a low or room temperature environment, the coefficient of thermal expansion $\alpha_x = -1.6\times10^{-6}\,K^{-1}$ (Murmu and Pradhan 2010) and for the high-temperature environment, the coefficient of thermal expansion is considered as $\alpha_x = 1.1\times10^{-6}\,K^{-1}$ (Murmu and Pradhan 2010). Fig. 1 depicts the variation of χ_{e_0a}, which is the ratio of frequency parameters using nonlocal theory and frequency parameters with local model, with small scale parameter e_0a whereas Fig. 2 represents the variations of first two frequency parameters with e_0a for different types of CNTs. It may be also noted that the frequency parameters for all types of CNTs for all modes are decreasing with the increase of small scale parameter. Another interesting observation is that fundamental frequency parameters for both the thermal environment follow the order as $(\lambda_1)_{\text{zigzag}} > (\lambda_1)_{\text{chiral}} > (\lambda_1)_{\text{armchair}}$ whereas for second mode frequency, $(\lambda_1)_{\text{armchair}} > (\lambda_1)_{\text{chiral}} > (\lambda_1)_{\text{Zigzag}}$.

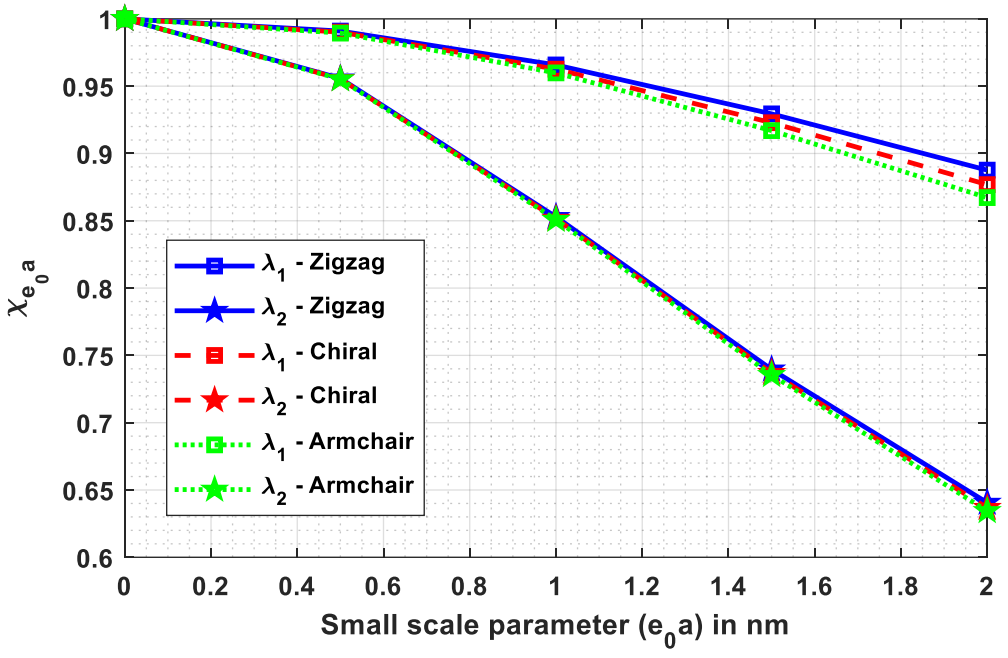

Fig. 1. $\chi_{e_0 a}$ Vs. $e_0 a$ (Low-Temperature Environment)

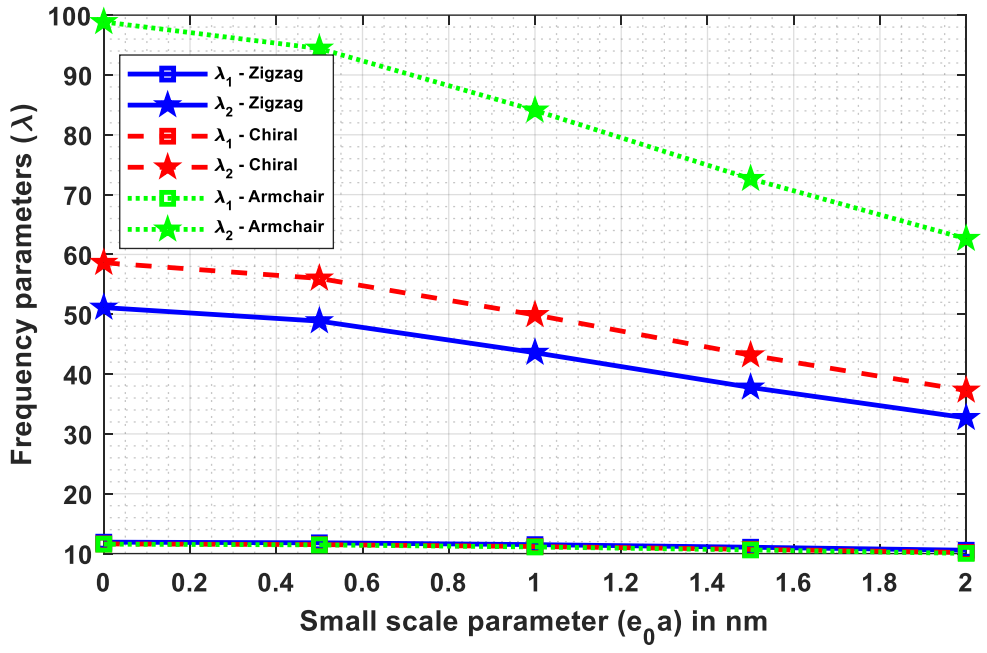

Fig. 2. λ Vs. $e_0 a$ (High-Temperature Environment)

4.3 Influence of change in temperature and thermal environment

The thermal environment and temperature changes (ΔT) influence the frequency parameters of CNTs significantly. In this regard, a parametric study has been carried out to investigate the impacts of temperature change and thermal environment on the first two-mode frequency parameters of armchair, chiral, and zigzag CNTs which are illustrated in Table 2 and Figs. 3-4. For this study, $k_w = 1GPa$, $L = 10nm$, and $e_0 a = 1nm$ have been taken along whereas ΔT is varying from 0 to 200 K with an increment of 50 K. Fig. 3 represents the variation of $\chi_{\Delta T}$, which is defined as the ratio of frequency parameters with temperature change and frequency parameters without any temperature changes, with ΔT for low-temperature environment whereas Fig. 4 depicts the variation for the high-temperature environment. From these results, it can be concluded that frequency parameters for all modes and all types of CNTs increase with the rise of ΔT for low-temperature environments and this trend is just opposite in the case of high-temperature environments. Another observation is that CNTs possess higher frequency parameters at room temperature than the high temperature environment.

Table 2 Non-dimensional frequency parameters $\lambda_n = \omega_n L^2 \sqrt{\frac{\rho A}{(EI)^{eff}}}$ with $k_w = 1GPa$, $L = 10nm$, and $e_0 a = 1nm$

(a) Low-temperature Environment $\left(\alpha_x = -1.6 \times 10^{-6} K^{-1}\right)$

ΔT	Zigzag		Chiral		Armchair	
	λ_1	λ_2	λ_1	λ_2	λ_1	λ_2
0	11.5133	43.6137	11.1902	49.9225	11.1157	84.1215
50	11.5249	43.6367	11.1997	49.9451	11.1232	84.1564
100	11.5366	43.6596	11.2092	49.9677	11.1306	84.1912
150	11.5482	43.6826	11.2187	49.9903	11.1381	84.2261
200	11.5598	43.7056	11.2282	50.0128	11.1456	84.2609

(b) High-temperature Environment $\left(\alpha_x = 1.1\times10^{-6}K^{-1}\right)$

e_0a	Zigzag		Chiral		Armchair	
	λ_1	λ_2	λ_1	λ_2	λ_1	λ_2
0	11.5133	43.6137	11.1902	49.9225	11.1157	84.1215
50	11.5052	43.5979	11.1836	49.9069	11.1106	84.0975
100	11.4972	43.5821	11.1771	49.8914	11.1054	84.0735
150	11.4892	43.5662	11.1705	49.8758	11.1003	84.0495
200	11.4811	43.5504	11.1640	49.8603	11.0951	84.0255

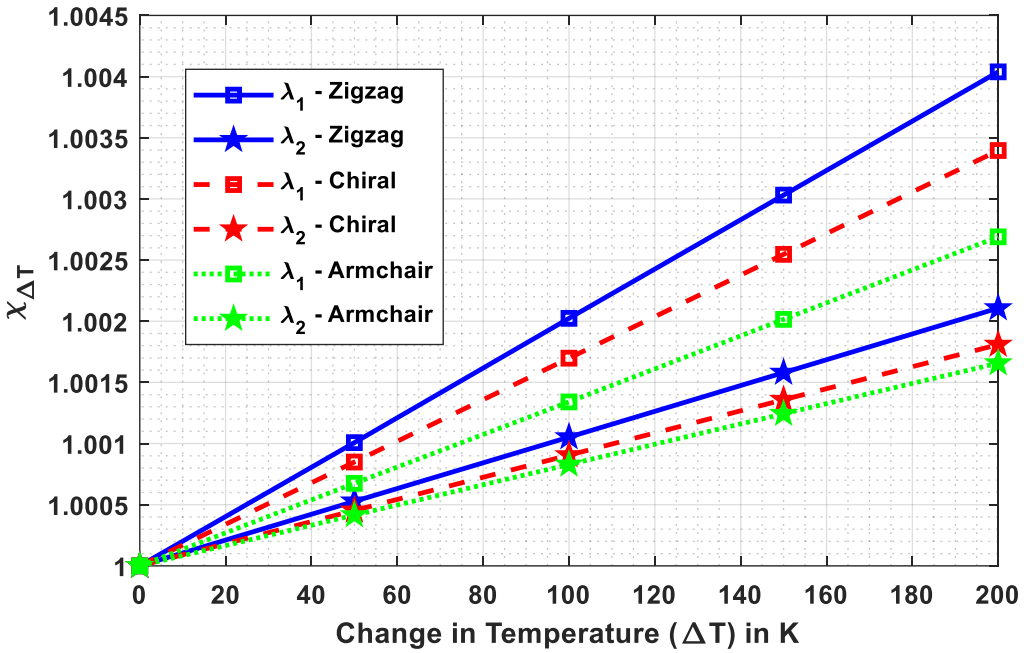

Fig. 3. $\chi_{\Delta T}$ Vs. ΔT (Low-Temperature Environment)

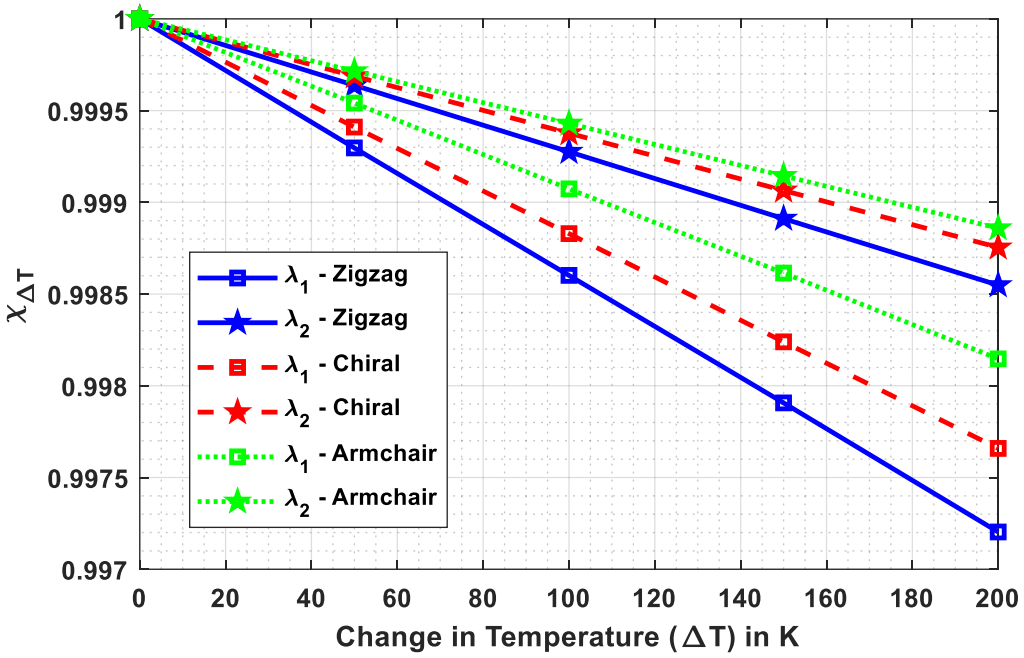

Fig. 4. $\chi_{\Delta T}$ Vs. ΔT (High-Temperature Environment)

4.4 Influence of elastic substrate

The influence of the Winkler modulus is investigated through this subsection which is illustrated in Table 3 and Figs. 5-6 with $\Delta T = 100K$, $L = 10nm$, and $e_0 a = 1nm$. Here the Winkler modulus (w_k) is taken as 0 to 4 GPa. The study is carried out for the first two-mode frequency parameters of armchair, chiral, and zigzag nanotubes. Table 3 represents the variation of frequency parameters with Winkler modulus (w_k), whereas Figs. 5-6 depict the variation of χ_{k_w}, which is defined as the ratio of frequency parameters with the elastic substrate and frequency parameters without an elastic substrate, with k_w. Frequency parameters for both the modes increase with the increase in Winkler modulus in both the environments.

Table 3 Frequency parameters $\lambda_n = \omega_n L^2 \sqrt{\frac{\rho A}{(EI)^{eff}}}$ with $\Delta T = 100K$, $L = 10nm$, and $e_0 a = 1nm$

(a) Low-temperature Environment $\left(\alpha_x = -1.6 \times 10^{-6} K^{-1}\right)$

k_w	Zigzag		Chiral		Armchair	
	λ_1	λ_2	λ_1	λ_2	λ_1	λ_2
0	10.1350	43.0054	10.2487	49.4184	10.5137	83.4880
1	11.5366	43.6596	11.2092	49.9677	11.1306	84.1912
2	12.7854	44.3043	12.0937	50.5110	11.7152	84.8887
3	13.9226	44.9396	12.9177	51.0485	12.2719	85.5804
4	14.9738	45.5661	13.6923	51.5804	12.8045	86.2666

(b) High-temperature Environment $\left(\alpha_x = 1.1\times10^{-6}K^{-1}\right)$

k_w	Zigzag		Chiral		Armchair	
	λ_1	λ_2	λ_1	λ_2	λ_1	λ_2
0	10.0902	42.9266	10.2135	49.3413	10.4869	83.3692
1	11.4972	43.5821	11.1771	49.8914	11.1054	84.0735
2	12.7499	44.2278	12.0639	50.4355	11.6912	84.7719
3	13.8901	44.8643	12.8899	50.9738	12.2491	85.4646
4	14.9435	45.4918	13.6660	51.5065	12.7826	86.1517

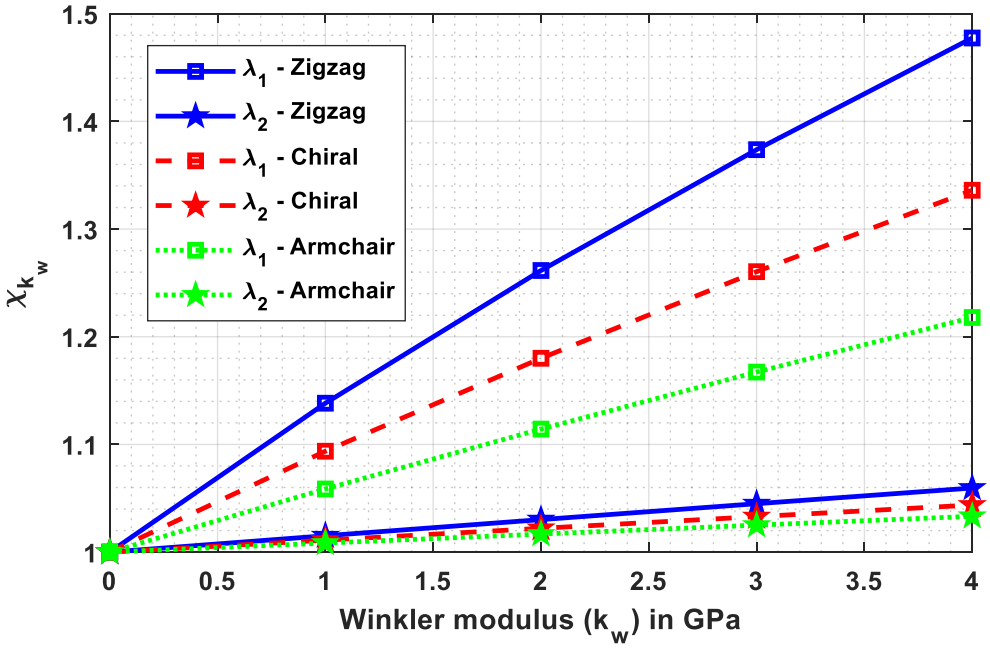

Fig. 5. χ_{k_w} Vs. k_w (Low-Temperature Environment)

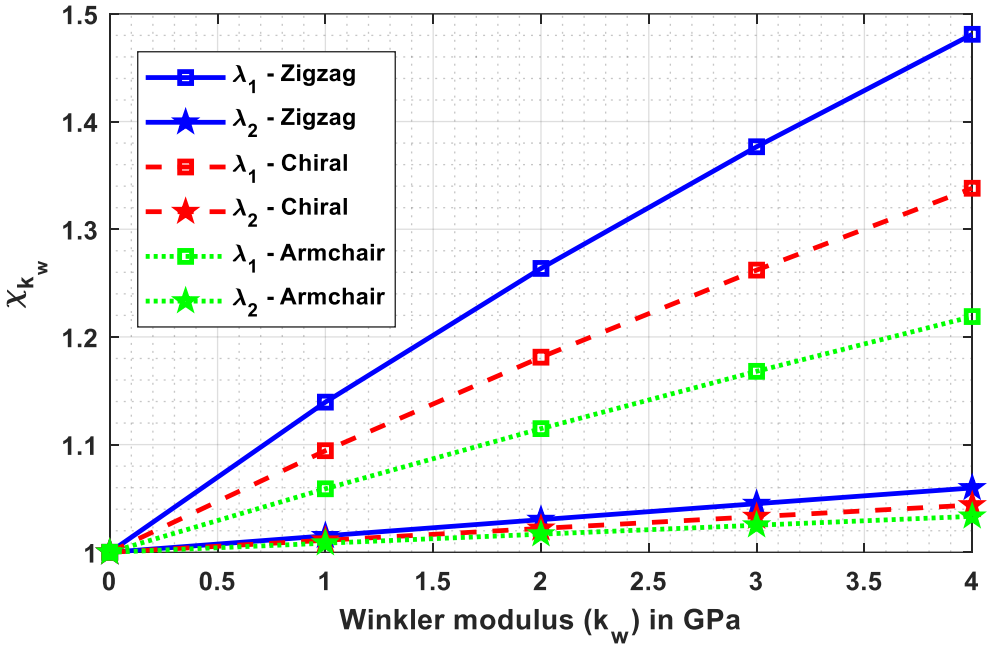

Fig. 6. χ_{k_w} Vs. k_w (High-Temperature Environment)

4.5 Influence of length of the CNTs

Investigation on the impact of length is very crucial as frequency parameters are affected by the size of the nanotubes. In order to analyze the response of the length parameter, we have considered $\Delta T = 100K$, $e_0 a = 1nm$ and $k_w = 1GPa$. Here the length of the nanotubes is assumed to vary from 10 nm to 30 nm with an increase of 5 nm. The first two modes of all the nanotubes which include armchair, zigzag, and chiral are considered for investigation in both the low and high-temperature environments which are displayed in Figs. 9-10 as graphical results. It is noticed that with the increase of length parameters, the fundamental frequency for all the CNTs and in both the environment increases whereas a random behavior has been observed in the case of second mode frequency.

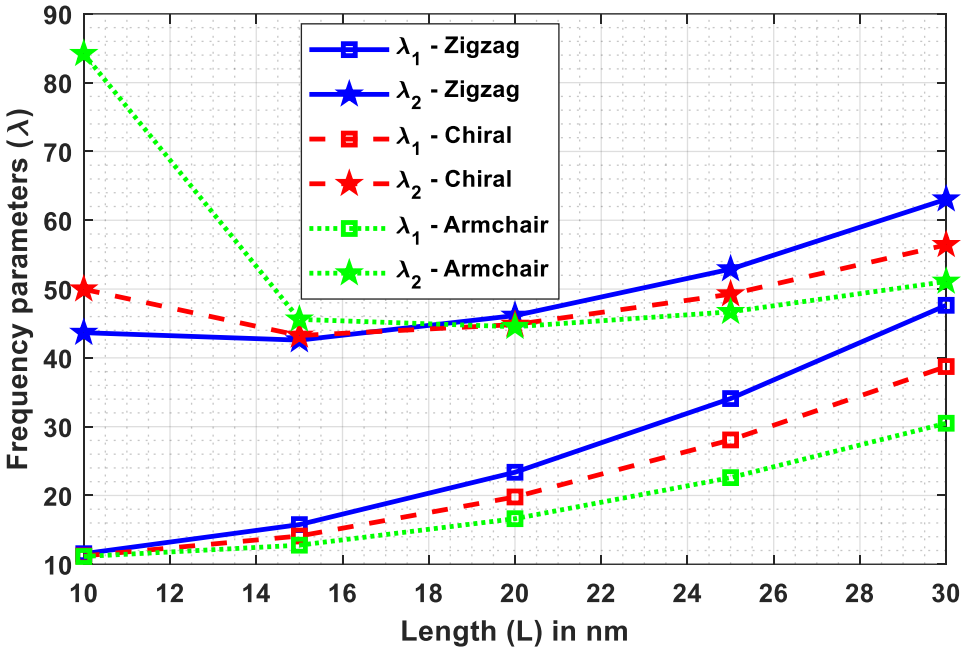

Fig. 7. λ Vs. L (Low-Temperature Environment)

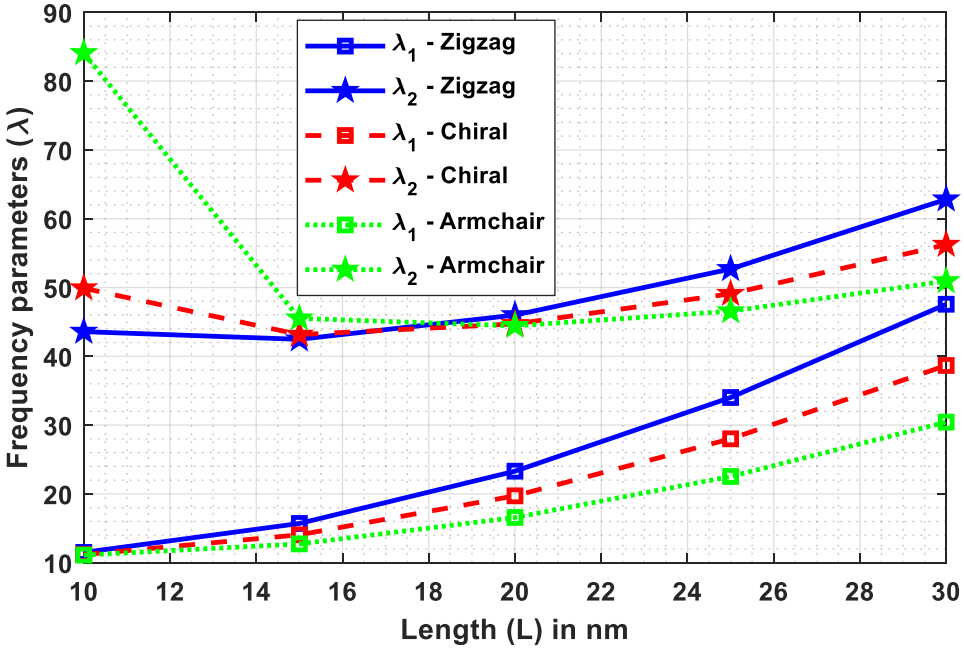

Fig. 8. λ Vs. L (High-Temperature Environment)

5 Conclusion

As this paper analyzes three geometric shapes of carbon nanotubes, and also as carbon nanotubes have been extensively studied in continuum models, this paper reveals that the study of all three

shapes is notable even in continuum conditions. In fact, most papers that considered carbon nanotubes by nonlocal continuum models used an averaged diameter to analyze the problem. The tendency to analyze all three shapes can be seen in molecular dynamic simulation only. In this regard, vibration characteristics of three different types of SWCNTs including armchair, chiral and zigzag have been explored, taking into account the impact of surface energy and surface residual stresses. The carbon nanotubes are also positioned in the elastic substrates of the Winkler type and subjected to both the low and high-temperature conditions. An analytical method, namely the Navier method, has been used to determine the analytical results for Pined-Pined (P-P) boundary conditions. Following are the main findings of the investigation;

- The frequency parameters of Armchair, chiral, and zigzag nanotubes are decreasing with the increase of small scale parameter. The fundamental frequencies for both the low and high-temperature environments follow the order as $(\lambda_1)_{\text{zigzag}} > (\lambda_1)_{\text{chiral}} > (\lambda_1)_{\text{armchair}}$ whereas for second mode frequency, the trend is changed as $(\lambda_1)_{\text{armchair}} > (\lambda_1)_{\text{chiral}} > (\lambda_1)_{\text{Zigzag}}$.
- The frequency parameters of first and second modes increase with the rise of ΔT for low-temperature environment and this trend is just opposite in case of high-temperature environment. Another observation is that CNTs possess higher frequency parameters at room or low temperature than the high-temperature environment.
- Frequency parameters increase with the increase in Winkler modulus in both the environments for both the modes.
- It is noticed that with the increase in length parameters, fundamental frequencies of all the CNTs increase in both the environments whereas a random behavior has been observed in the case of second mode frequency.

Acknowledgment

The first two authors are very much thankful to Defence Research & Development Organization (DRDO), New Delhi, India (Sanction Code: DG/TM/ERIPR/GIA/17-18/0129/020) for the funding to carry out the present research work.

References

Abualnour, M., A. Chikh, H. Hebali, A. Kaci, A. Tounsi, A. A. Bousahla, and A. Tounsi. 2019. Thermomechanical analysis of antisymmetric laminated reinforced composite plates using a new four variable trigonometric refined plate theory. *Computers and Concrete* 24(6):489-498.

Adim, B., T. H. Daouadji, B. Abbes, and A. Rabahi. 2016. Buckling and free vibration analysis of laminated composite plates using an efficient and simple higher order shear deformation theory. *Mechanics & Industry* 17(5):512.

Adim, B. and T. H. Daouadji. 2016. Effects of thickness stretching in FGM plates using a quasi-3D higher order shear deformation theory. *Advances in materials Research 5*(4):223-244.

Alimirzaei, S., M. Mohammadimehr, A. Tounsi. 2019. Nonlinear analysis of viscoelastic micro-composite beam with geometrical imperfection using FEM: MSGT electro-magneto-elastic bending, buckling and vibration solutions. *Structural Engineering and Mechanics* 71(5):485-502.

Arefi, Mohammad, and Amir Hossein Soltan Arani. 2018. Higher order shear deformation bending results of a magnetoelectrothermoelastic functionally graded nanobeam in thermal, mechanical, electrical, and magnetic environments. *Mechanics Based Design of Structures and Machines* 46(6):669-692.

Bedia, W. A., M. S. Houari, A. Bessaim, A. A. Bousahla, A. Tounsi, T. Saeed, and M. S. Alhodaly. 2019. A New Hyperbolic Two-Unknown Beam Model for Bending and Buckling Analysis of a Nonlocal Strain Gradient Nanobeams. *Journal of Nano Research* 57:175-191.

Belbachir, N., K. Draich, A. A. Bousahla, M. Bourada, A. Tounsi, M. Mohammadimehr. 2019. Bending analysis of anti-symmetric cross-ply laminated plates under nonlinear thermal and mechanical loadings. *Steel and Composite Structures*, 33(1):81-92.

Bensattalah, T., M. Zidour, T. H. Daouadji, and K. Bouakaz. 2019. Theoretical analysis of chirality and scale effects on critical buckling load of zigzag triple walled carbon nanotubes under axial compression embedded in polymeric matrix. *Structural Engineering and Mechanics* 70(3): 269-277.

Bensattalah, T., M. Zidour, and T. H. Daouadji. 2018. Analytical analysis for the forced vibration of CNT surrounding elastic medium including thermal effect using nonlocal Euler-Bernoulli theory. *Advances in materials Research 7*(3):163-174.

Berghouti, H., E. A. Adda Bedia, A. Benkhedda, and A. Tounsi. 2019. Vibration analysis of nonlocal porous nanobeams made of functionally graded material. *Advances in nano research* 7(5):351-364.

Boutaleb, S., K. H. Benrahou, A. Bakora, A. Algarni, A. A. Bousahla, A. Tounsi, A. Tounsi, and S. R. Mahmoud. 2019. Dynamic analysis of nanosize FG rectangular plates based on simple nonlocal quasi 3D HSDT. *Advances in nano research* 7(3):191-208.

Dastjerdi, S. and Y. Tadi Beni. 2019. A novel approach for nonlinear bending response of macro-and nanoplates with irregular variable thickness under nonuniform loading in thermal environment. *Mechanics Based Design of Structures and Machines* 1-26.

Draoui, A., M. Zidour, A. Tounsi, and B. Adim. 2019. Static and Dynamic Behavior of Nanotubes-Reinforced Sandwich Plates Using (FSDT). *Journal of Nano Research* 57:117-135.

Farshi, B., A. Assadi, and A. Alinia-Ziazi. 2010. Frequency analysis of nanotubes with consideration of surface effects. *Applied Physics Letters* 96:093105.

Fattahi, A. M., S. Sahmani, and N. A. Ahmed. 2019. Nonlocal strain gradient beam model for nonlinear secondary resonance analysis of functionally graded porous micro/nano-beams under periodic hard excitations. *Mechanics Based Design of Structures and Machines* 1–30.

Ghavanloo, E., and S. A. Fazelzadeh. 2012. Vibration characteristics of single-walled carbon nanotubes based on an anisotropic elastic shell model including chirality effect. *Applied Mathematical Modelling* 36:4988-5000.

Hussain, M., M. N. Naeem, A. Tounsi, and M. Taj. 2019. Nonlocal effect on the vibration of armchair and zigzag SWCNTs with bending rigidity. *Advances in Nano Research 7*(6):431-442.

Jena, S. K., and S. Chakraverty. 2019. Dynamic Behavior of Electro-Magnetic Nanobeam Using Haar Wavelet Method (HWM) and Higher Order Haar Wavelet Method (HOHWM). *The European Physical Journal Plus* 134(10):538.

Jena, S. K., S. Chakraverty, and F. Tornabene. 2019a. Buckling Behavior of Nanobeam Placed in an Electro-Magnetic Field Using Shifted Chebyshev polynomials Based Rayleigh-Ritz Method. *Nanomaterials* 9(9): 1326.

Jena, S. K., S. Chakraverty, and F. Tornabene. 2019b. Vibration characteristics of nanobeam with exponentially varying flexural rigidity resting on linearly varying elastic foundation using differential quadrature method. *Materials Research Express* 6(8): (085051)1-13.

Jena, S. K., S. Chakraverty, and F. Tornabene. 2019c. Dynamical Behavior of Nanobeam Embedded in Constant, Linear, Parabolic and Sinusoidal Types of Winkler Elastic Foundation Using First-Order Nonlocal Strain Gradient Model. *Materials Research Express* 6(8): (0850f2)1-23.

Jena, S. K., S. Chakraverty, and R. M. Jena. 2019. Propagation of Uncertainty in Free Vibration of Euler-Bernoulli Nanobeam. *Journal of the Brazilian Society of Mechanical Sciences and Engineering* 41(10): 436.

Jena, S. K., S. Chakraverty, and M. Malikan. 2019. Implementation of Haar wavelet, higher order Haar wavelet, and differential quadrature methods on buckling response of strain gradient nonlocal beam embedded in an elastic medium. *Engineering with Computers* doi.org/10.1007/s00366-019-00883-1.

Jena, S. K., S. Chakraverty, M. Malikan, and F. Tornabene. 2019. Stability analysis of single-walled carbon nanotubes embedded in winkler foundation placed in a thermal environment considering the surface effect using a new refined beam theory. *Mechanics Based Design of Structures and Machines, An International Journal* doi.org/10.1080/15397734.2019.1698437.

Jena, S. K., S. Chakraverty, and M. Malikan. 2020a. Vibration and buckling characteristics of nonlocal beam placed in a magnetic field embedded in Winkler–Pasternak elastic foundation using a new refined beam theory: an analytical approach. *European Physical Journal Plus* 135(2):1-18.

Jena, S. K., S. Chakraverty, and M. Malikan. 2020b. Implementation of non-probabilistic methods for stability analysis of nonlocal beam with structural uncertainties. *Engineering with Computers* 1-13.

Jena, S. K., and S. Chakraverty. 2018. Free vibration analysis of Euler-Bernoulli Nano beam using differential transform method. *International Journal of Computational Materials Science and Engineering* 7:1850020.

Jiang, J., L. Wang, and Y. Zhang. 2017. Vibration of Single-Walled Carbon Nanotubes with Elastic Boundary Conditions. *International Journal of Mechanical Sciences* 122:156-166.

Karami, B., M. Janghorban, A. Tounsi. 2019a. On exact wave propagation analysis of triclinic material using three-dimensional bi-Helmholtz gradient plate model. *Structural Engineering and Mechanics*, 69(5):487-497.

Karami, B., M. Janghorban, A. Tounsi. 2019b. Wave propagation of functionally graded anisotropic nanoplates resting on Winkler-Pasternak foundation. *Structural Engineering and Mechanics* 70(1): 55-66.

Karami, B., M. Janghorban, and A. Tounsi. 2019c. Galerkin's approach for buckling analysis of functionally graded anisotropic nanoplates/different boundary conditions. *Engineering with Computers* 35(4):1297-316.

Karami, B., D. Shahsavari, M. Janghorban, A. Tounsi. 2019. Resonance behavior of functionally graded polymer composite nanoplates reinforced with graphene nanoplatelets. *International Journal of Mechanical Sciences* 156:94-105.

Larbi, L.O., A. Kaci, M. S. A. Houari, and A. Tounsi. 2013. An efficient shear deformation beam theory based on neutral surface position for bending and free vibration of functionally graded beams. *Mechanics Based Design of Structures and Machines* 41(4):421-433.

Lee, H. L., and W. J. Chang. 2010. Surface effects on frequency analysis of nanotubes using nonlocal Timoshenko beam theory. *Journal of Applied Physics* 108:093503.

Mahmoudi, A., S. Benyoucef, A. Tounsi, A. Benachour, E. A. Adda Bedia, and S. R. Mahmoud. 2019. A refined quasi-3D shear deformation theory for thermo-mechanical behavior of functionally graded sandwich plates on elastic foundations. *Journal of Sandwich Structures & Materials* 21(6):1906-29.

Malikan, M., V. B. Nguyen, and F. Tornabene. 2018. Damped forced vibration analysis of single-walled carbon nanotubes resting on viscoelastic foundation in thermal environment using nonlocal strain gradient theory. *Engineering Science and Technology, an International Journal* 21:778-786.

Malikan, M. 2019. On the buckling response of axially pressurized nanotubes based on a novel nonlocal beam theory. *Journal of Applied and Computational Mechanics* 5 :103-112.

Malikan, M., R. Dimitri, and F. Tornabene. 2019. Transient response of oscillated carbon nanotubes with an internal and external damping. *Composites Part B: Engineering* 158:198-205.

Malikan, M. and V. A. Eremeyev. 2020. Post-critical buckling of truncated conical carbon nanotubes considering surface effects embedding in a nonlinear Winkler substrate using the Rayleigh-Ritz method. *Materials Research Express*. https://doi.org/10.1088/2053-1591/ab691c

Malikan, M., M. Krasheninnikov, and V. A. Eremeyev. 2020. Torsional stability capacity of a nano-composite shell based on a nonlocal strain gradient shell model under a three-dimensional magnetic field. *International Journal of Engineering Science* 148:103210.

Medani, M., A. Benahmed, M. Zidour, H. Heireche, A. Tounsi, A. A. Bousahla, A. Tounsi, and S. R. Mahmoud. 2019. Static and dynamic behavior of (FG-CNT) reinforced porous sandwich plate using energy principle. *Steel and Composite Structures* 32(5):595-610.

Murmu, T., and S. C. Pradhan. 2010. Thermal effects on the stability of embedded carbon nanotubes. *Computational Materials Science* 47:721-7.

Reddy, J.N. 2007. Nonlocal theories for bending, buckling and vibration of beams. *International Journal of Engineering Science* 45:288-307.

Semmah, A., H. Heireche, A. A. Bousahla, and A. Tounsi. 2019. Thermal buckling analysis of SWBNNT on Winkler foundation by non-local FSDT. *Advances in nano research 7*(2):89-98.

Tlidji, Y., M. Zidour, K. Draiche, A. Safa, M. Bourada, A. Tounsi, A. A. Bousahla, S. R. Mahmoud. 2019. Vibration analysis of different material distributions of functionally graded microbeam. *Structural Engineering and Mechanics* 69(6):637-649.

Zarga, D., A. Tounsi, A. A. Bousahla, F. Bouradaand, S. R. Mahmoud. 2019. Thermomechanical bending study for functionally graded sandwich plates using a simple quasi-3D shear deformation theory. *Steel and Composite Structures* 32(3):389-410.

Zhang, M., and J. Li. 2009. Carbon nanotube in different shapes. *Materials today* 12:12-18.

Zhen, Y. X. 2017. Wave propagation in fluid-conveying viscoelastic single-walled carbon nanotubes with surface and nonlocal effects. *Physica E: Low-dimensional Systems and Nanostructures* 86:275-279.